

Interaction of CO with Pd clusters supported on a thin alumina film

A. Sandell and J. Libuda

Lehrstuhl für Physikalische Chemie I, Ruhr-Universität Bochum, D-44780 Bochum, Germany

P. A. Brühwiler, S. Andersson, and A. J. Maxwell

Department of Physics, Uppsala University, Box 530, S-751 21 Uppsala, Sweden

M. Bäumer

Lehrstuhl für Physikalische Chemie I, Ruhr-Universität Bochum, D-44780 Bochum, Germany

N. Mårtensson

Department of Physics, Uppsala University, Box 530, S-751 21 Uppsala, Sweden

H. J. Freund

Lehrstuhl für Physikalische Chemie I, Ruhr-Universität, Bochum, D-44780 Bochum, Germany

(Received 2 October 1995; accepted 12 February 1996)

The adsorption of CO on Pd particles supported on a thin alumina film has been studied employing high resolution x-ray photoelectron spectroscopy (XPS) and x-ray absorption spectroscopy (XAS), and of special interest was the CO–Pd interaction as a function of island size and CO coverage. CO saturation at 90 K leads to an overlayer characterized by a rather weak CO–Pd hybridization as manifested by the core ionized and core excited states. The interaction strength gradually increases with island size. Desorption of parts of the overlayer results in CO more strongly interacting with the Pd islands. A comparison between the XPS and XAS energies yields a behavior indistinguishable from metallic systems for islands larger than 15 Å, i.e., the XPS binding energy appears near the x-ray absorption onset. For the smallest islands (5 Å), a CO coverage dependent reversal of the XPS–XAS energy relation was observed, indicating a drastic change in the screening ability of the CO–Pd complex. © 1996 American Vacuum Society.

I. INTRODUCTION

Oxide-supported metal particles are systems which have attracted a lot of attention because of their catalytic activity. The need for a fundamental understanding of the catalyst in itself as well as the elementary processes involved in the adsorption and decomposition of small molecules, such as CO, motivates the application of sophisticated surface science techniques. However, studies of the industrially manufactured catalysts are not easy to perform due to their amorphous structure and, since oxides are insulators, problems with charging may also occur when employing electron spectroscopies. In order to avoid these problems, different model systems better suited for surface science studies have been developed, e.g., Refs. 1–3.

One example is a thin, ordered Al₂O₃ oxide film grown upon NiAl(110), which has previously been used as a substrate for deposits of metals.^{4–9} In particular, the cluster growth of Pd has been investigated with various techniques, such as spot-profile analysis low-energy electron diffraction (SPA-LEED), photoelectron spectroscopy (PES), and thermal desorption spectroscopy (TDS).^{7–9} Pd was found in all cases to form three-dimensional (3D) islands, but significant differences in growth depending on deposition conditions (e.g. the substrate temperature) were observed. Further, the CO adsorption properties were found to strongly depend on cluster size. For example, TDS shows an increased tendency for desorption at lower temperatures for smaller clusters.⁸ The TD spectra for the small clusters differs substantially from those obtained for CO adsorbed on Pd single crystals.¹⁰

Thus, molecules adsorbed on the supported metal particles may exhibit properties which are very different from the ones for molecules adsorbed on the corresponding bulk metal.

Core level spectroscopies have previously proven to be most powerful tools in studies of adsorbates because of the high surface sensitivity and atomic selectivity, and, provided that the resolution is high enough, detailed information regarding the chemical state, adsorption geometries, interaction strengths, etc., can be obtained.¹¹ Therefore, we have chosen as a next step to study the adsorption of CO on Pd particles deposited on Al₂O₃/NiAl(110) using high resolution x-ray photoelectron spectroscopy (XPS) and x-ray absorption spectroscopy (XAS). Of special interest is the CO–Pd interaction as a function of particle size and CO coverage.

II. EXPERIMENT

The experiments were carried out at beamline 22 at the Swedish synchrotron radiation facility MAX Lab in Lund. The setup contains a modified Zeiss SX-700 monochromator in conjunction with a large hemispherical electron energy analyzer for photoemission and a multichannel plate with a retarding grid for x-ray absorption measurements by detection of secondary electrons.¹² The C 1s XP spectra were recorded at a photon energy of 380 eV with a total resolution set to 0.4 eV. The Pd 3d XP spectra were recorded at a photon energy of 420 eV and a resolution of 0.3 eV. All the XPS binding energies are referred to the Fermi level of the NiAl(110) substrate. The XA spectra were measured in par-

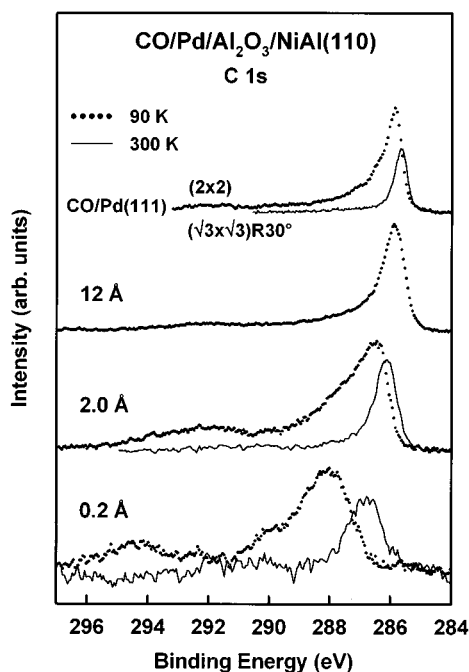


FIG. 1. C 1s photoelectron spectra for CO adsorbed at 90 K on Pd clusters of increasing size before and after heating to 300 K, compared to CO/Pd(111) (2 \times 2) and ($\sqrt{3}\times\sqrt{3}$)R30°. The spectra are normalized to the background level in order to show the decrease in C 1s intensity due to desorption.

tial yield mode with a photon energy resolution of 0.2 eV at both the C 1s and the O 1s edges. Fortunately, the CO-related O 1s XAS peaks were easy to separate from the oxide features, thereby allowing for a subtraction of the oxide features. The absolute photon energies (PE) were determined using photoemission spectra excited by first- and second-order radiation.

The preparation of the clean NiAl(110) surface and the oxidation procedure to form a well-ordered Al₂O₃ film have been extensively described elsewhere.³ Pd was evaporated using a Knudsen cell and the evaporation rate was monitored using a quartz microbalance. With the use of SPA-LEED, the following approximate average island sizes could be estimated: 5 and 15 Å for 0.2 and 2.0 Å Pd deposited at 90 K, respectively, and about 50 Å for 12 Å deposited at 300 K.^{7,8} We will use the nominal film thicknesses as obtained by the quartz microbalance to denote the different situations.

III. RESULTS AND DISCUSSION

A. Adsorption at 90 K

Figure 1 shows C 1s XP spectra for 30 L CO adsorbed at 90 K on increasing amounts of Pd: 0.2 and 2.0 Å deposited at a sample temperature of 90 K and 12 Å deposited at 300 K. Adsorption of large amounts of CO at 90 K on Pd(111) leads to the formation of a (2 \times 2) overlayer, and a spectrum representing this situation, recorded with slightly higher resolution, is shown at the top of Fig. 1 for comparison (from Ref. 13). No O 1s spectra for the supported islands are shown, since the strong oxide signal was found to obscure

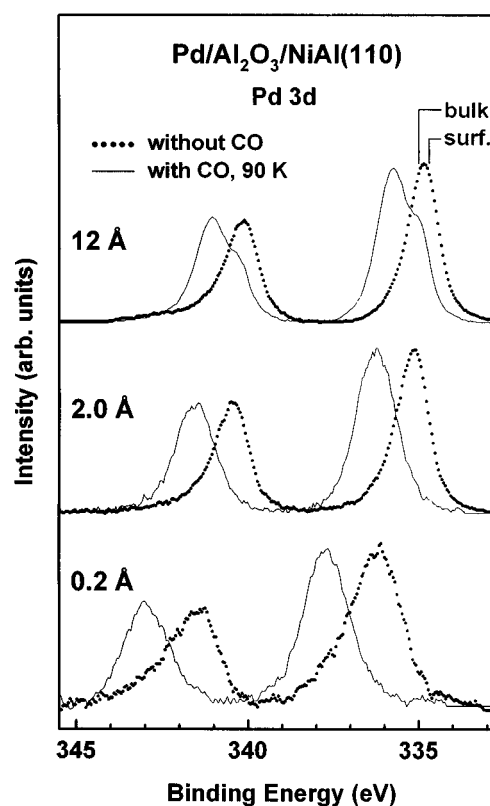


FIG. 2. Pd 3d photoelectron spectra for the different Pd exposures with and without CO adsorbed. A simple integrated background has been subtracted and the spectra are normalized to the peak maxima.

the CO-induced features. In Fig. 2, we show the corresponding influence on the Pd 3d peaks upon CO adsorption.

1. Size-dependent binding-energy shifts

Starting with the binding-energy (BE) shifts, the Pd core levels shown in Fig. 2 exhibit a successive shift toward lower values for increasing island sizes, which is a typical property for the growth of metal clusters on inert substrates.¹⁴⁻¹⁷ The shifts can be attributed to several different effects, which are most difficult to separate. First, there are initial state effects caused by rehybridizations due to interactions between atoms within the cluster and between the cluster and the substrate. Second, final state effects have to be considered, such as the possibility of a charge left on the cluster due to inefficient screening from the substrate and changes in the ability of the cluster to provide local screening. Several of these effects can be expected to be similar for adsorbates bonded to clusters, which is consistent with the related behavior seen in Fig. 1.^{18,19}

For large metal exposures, the BEs, of course, reach the bulk metal values. In fact, SPA-LEED results show that the deposition of large amounts of Pd at 300 K results in particles dominated by (111) facets.⁸ This is confirmed by the tremendous similarity between the CO/12 Å spectrum and the CO/Pd(111) (2 \times 2) spectrum.

2. Size-dependent XPS line-broadening effects

The core-level line profiles for small clusters can be influenced by a number of different broadening effects. The

distribution of sites occupied by the clusters on the support is expected to cause a broadening which increases with decreasing cluster size.¹⁷ The island size distribution also induces a broadening, and effects due to cluster atoms in inequivalent positions may also occur. The linewidth, not only the BE, is furthermore strongly dependent on the screening processes. Calculations show that a broadening is expected to occur if the valence bandwidth decreases,^{20,21} and PES results indeed show a valence-band narrowing for decreasing cluster sizes.^{9,14,17} Moreover, the photoemission process may lead to vibrational excitations and shakeups, which also may involve the support. Finally, in the case of molecules adsorbed on the clusters, additional effects will occur, which will be further discussed below.

Regarding the present situations, the components in the Pd 3*d* spectra for 2 Å Pd have widths similar to the bulk metal case (12 Å Pd), whereas the peaks in the 0.2 Å spectra are significantly broader (Fig. 2). Thus, the linewidth for the 2 Å case is probably dominated by the same processes as for the metal, whereas the broadening effects mentioned above may be present for the 0.2 Å situation.

3. The CO adsorption sites

When discussing differences in line profiles and BEs found in core level spectra for clusters with adsorbates, it is important to consider the adsorption geometries. A population of different CO adsorption sites has been found to induce C 1*s* BE shifts of the order of 0.5–1 eV.^{22,23} The (2×2) phase of CO/Pd(111) has been proposed to consist of molecules adsorbed in both threefold hollow and on-top positions.^{24,25} This mixture of adsorption sites is consistent with the appearance of a main peak with a high BE shoulder observed in the C 1*s* spectrum (Fig. 1), and, in line with previous results, where the component with the lowest BE can be assigned to the most highly coordinated site.^{13,22,23}

The adsorption of CO also shifts the substrate surface components toward higher BEs, an amount dependent on the coordination of metal atoms to CO.^{23,26} In the case of Pd(111), a surface core level shift of –0.3 eV has been found and this spectrum is identical to the clean 12 Å situation.²⁷ Upon CO saturation at 90 K, we find in Fig. 2 that a strong bulk component at 335.0 eV remains, whereas the surface component at 334.7 eV completely disappears, i.e., all surface atoms coordinate to CO.

In the case of the smaller clusters, the islands formed by deposition at 90 K are poorly ordered, which precludes a detailed site analysis.⁸ The Pd 3*d* data exhibit large shifts toward higher BEs upon CO adsorption for both 0.2 and 2 Å (Fig. 2), and the most important result for these two situations is that there is no or very little nonsurface Pd; for 0.2 Å no bulk component is found, whereas the intensity of a bulk feature in the 2 Å case can be estimated to be 7% ± 3%. We note that the asymmetry on the high BE side observed for 0.2 Å Pd before CO saturation is caused by contamination by small amounts of CO.

Turning next to the C 1*s* results, the lack of well-defined adsorption sites implies that the saturated CO overlayer may

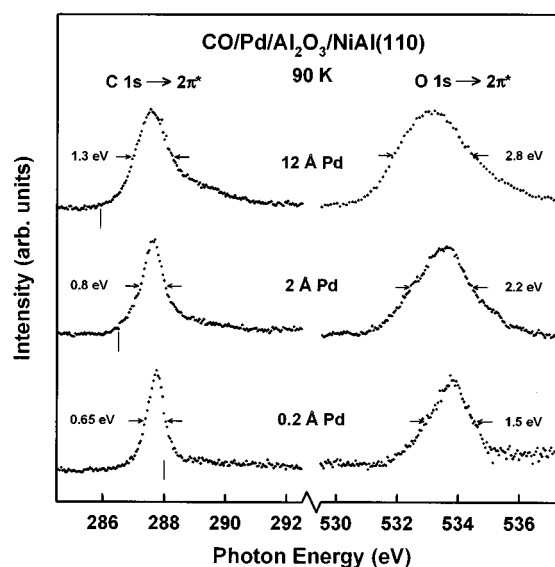


Fig. 3. X-ray absorption spectra for CO adsorbed on Pd clusters of increasing size. The lines in the C 1*s* XA spectra represent the XPS binding energies.

consist of CO adsorbed in a multitude of sites, leading to a more or less continuous distribution of C 1*s* BEs. Furthermore, the relative amounts of CO in different sites is expected to vary with size and shape of the cluster. These effects could account for line shapes which strongly deviate from those found for CO/Pd(111). For 0.2 Å, the broadening mechanisms mentioned in Sec. III A 2 may also play a role, but a major issue when discussing features and line profiles in the CO core-level spectra for all cluster sizes is the shake-up intensity and this will be elaborated in the following section.

4. The CO–Pd interaction strength and screening properties

Variations in the shake-up intensity in the XP spectra for chemisorbed CO have been widely discussed and are generally believed to be related to variations in the interaction strength between the substrate and the molecule.^{18,19,28,29} In systems where CO adsorbs weakly, strong satellites have been observed, whereas the satellite intensity for strongly bonded CO is significantly lower. Thus, variations in the shake-up intensity occur depending both on the substrate and the adsorption site. The shake-up intensity for the CO-saturated islands, see Fig. 1, is found to increase with decreasing Pd exposure, and indicates that the CO–Pd interaction strength decreases with decreasing island size. This interpretation is supported by TD spectra.⁸

Further information regarding the adsorbate–substrate interaction can be derived from the XAS results, which are presented in Fig. 3. The most notable effect is that the widths of the peaks increase with Pd exposure. The width of the π resonance has been argued to reflect the adsorbate–substrate hybridization strength between the CO 2*π** orbital and the metal states of the core excited state rather than the ground

state.^{30,31} Thus, for the saturated overlayer, the CO $2\pi^*$ -Pd $4d$ hybridization width of the core excited states is found to increase with island size, which in fact is the same trend as for the ground state as monitored by TDS and the shake-up intensities.

Moreover, by comparing the XPS and XAS data, information regarding the screening properties can be obtained. The relation between the XPS BE relative to the substrate Fermi level and the energy position of the x-ray absorption edge has been carefully determined for a number of chemisorption systems.^{31,32} It was found, without exceptions, that the XPS BE always appear near the onset of the XA peak. This connection is an effect of the hybridization between the electronic levels of the adsorbate and the metal, thereby allowing for metallic screening of the core ionized molecule.³² The XPS component with the lowest BE corresponds to the core ionized state where an electron has been transferred to the Fermi level. Since the states at E_F overlap with the adsorbate levels due to the hybridization, an efficient screening of the core hole situated on the molecule is provided. Consequently, the XPS BE defines the Fermi level in the XA spectrum and is thus bound to appear in connection with the onset of the absorption edge.

However, for a system where the adsorbate is not chemically bonded to the substrate, this connection is no longer valid. No electron transfer to the adsorbate occurs on the time scale of the photoionization process due to the almost negligible overlap between the levels of the adsorbate and the substrate.³³ Hence there is no such simple relationship between the energies of the core ionization and core excitation processes.

In Fig. 3, the C $1s$ BEs relative to the Fermi level are marked with lines, and it is observed that whereas the energy of the XA peaks remain essentially constant, the XPS BE gradually moves from a position slightly above the XA maximum (0.2 Å) to a position at the XA onset (12 Å). In order to explain this behavior, we have to consider that the CO molecules are chemically bonded to the Pd atoms and it is therefore appropriate to treat the whole CO/Pd complex as an adsorbate on the oxide film. For very large amounts of Pd, the situation of course approaches CO adsorption on bulk Pd. This is corroborated by the XPS-XAS relation for 12 Å, i.e., the XPS BE appears at the XA onset.

This is in contrast to the 0.2 Å situation, where previous PES results indicate that the islands lack the properties of an extended, metallic system.⁹ CO adsorbed on these small islands can therefore be regarded as similar to carbonyl molecules on an oxide, and the XPS BE is consequently not expected to be strictly connected to the XAS onset. We find that this is the case for CO/0.2 Å Pd at CO saturation, since the XPS BE appears slightly above the XAS peak.

The islands formed by deposition of 2 Å Pd represent an intermediate situation: PES shows a broad $4d$ band,⁹ and the core levels are shifted toward higher BEs as compared to the bulk metal. The XPS BE appears below the XA maximum, but not quite as near to the onset as in the 12 Å case.

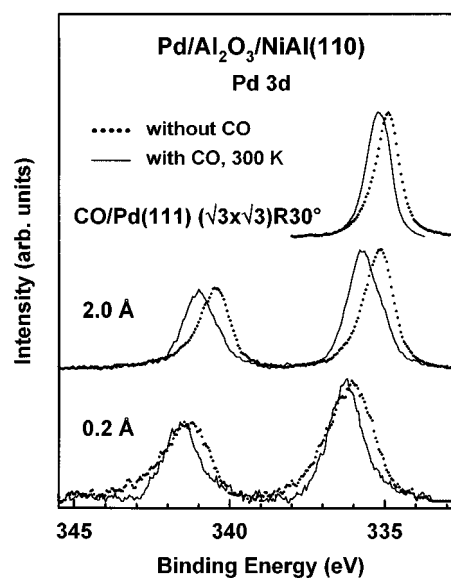


FIG. 4. Pd $3d$ photoelectron spectra for two different Pd exposures after heating the CO overlayer to 300 K compared to the clean situations. A simple integrated background has been subtracted from each spectrum.

B. Heating of the CO overlayer to 300 K

In order to investigate effects due to differences in CO coverage on the islands formed by deposition of 0.2 and 2 Å Pd, the overlayer was heated to 300 K, which resulted in desorption of $60\% \pm 5\%$ of the CO molecules in both cases. In this context it is important to note that heating to 300 K does not drastically change the size or structure of the Pd islands; CO saturation at 90 K of the heated islands regains the initial situation. The C $1s$ spectra for the low coverage situations are shown in Fig. 1. For comparison, the spectrum representing the CO/Pd(111) $(\sqrt{3} \times \sqrt{3})R30^\circ$ phase is shown.¹³ This structure can be formed by desorption of 56% of the (2×2) overlayer by heating. The corresponding Pd $3d$ spectra are presented in Fig. 4.

1. Adsorption sites at low CO coverage

The $(\sqrt{3} \times \sqrt{3})R30^\circ$ phase has been shown to consist of CO only adsorbed in hollow sites.^{24,25,34} In Fig. 1 it can be seen that this results in a more narrow C $1s$ peak which is shifted 0.2 eV toward lower BE. The changes in the C $1s$ line can be explained by occupation of only one site in contrast to the (2×2) situation where at least two different sites are populated, and by decreased CO-CO repulsion. On the Pd(100) surface, where only bridge sites are populated, it was found that compression of the overlayer induces a C $1s$ BE increase of 0.2 eV, which provides an estimate of the repulsion effect.³¹ The $(\sqrt{3} \times \sqrt{3})R30^\circ$ phase furthermore induces a smaller Pd $3d$ shift as compared to the (2×2) phase (see Figs. 2 and 4), which is consistent with a decrease in the coordination of Pd with CO.¹³

If we turn to the supported clusters, CO on the 0.2 and 2 Å Pd situations undergo the same overall changes upon heating: The C $1s$ line narrows considerably and the remaining

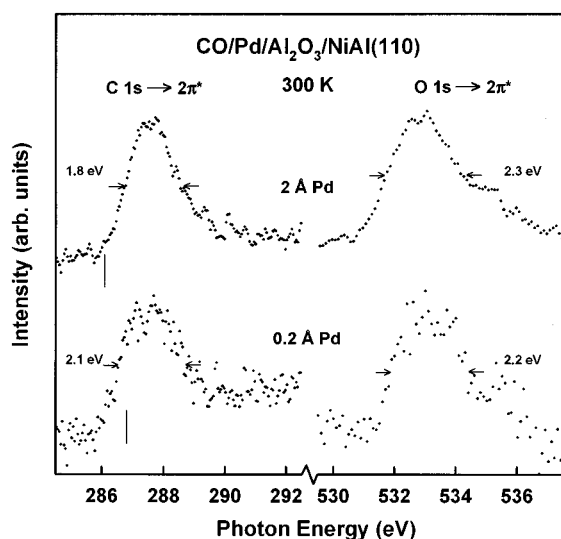


Fig. 5. X-ray absorption spectra for CO adsorbed on two different cluster sizes after heating to 300 K. The lines in the C 1s XA spectra represent the XPS binding energies.

peak has a lower BE. The smaller CO-induced Pd 3d shift (Fig. 4) gives further support for an overlayer with a lower Pd coordination to CO.

The question now is whether the species left after heating of the clusters was also present before heating. The C 1s peak in the 2 Å spectrum shifts 0.3 eV toward lower BE, which is of the same order as the effects induced by CO–CO repulsion. It can therefore not be excluded that this species also exists in the CO saturated case. The shift in the C 1s spectrum for 0.2 Å is of the order of 1.2 eV, which would suggest that this species was absent before heating, but in this particular case the C 1s shift is strongly influenced by the screening ability of the CO–Pd complex, which will be further discussed in the following section.

2. The CO–Pd interaction strength and screening properties at low CO coverage

The satellite intensity in the C 1s spectra are found to decrease upon removal of CO, indicating a stronger CO–Pd interaction strength for the remaining species. The shake-up intensity, however, is also correlated to the CO adsorption sites, and decreases for sites with increasing coordination.²⁹

The XA spectra are shown in Fig. 5, and the C 1s XA peaks are found to broaden considerably upon heating of the CO overlayer, i.e., the $2\pi^*-4d$ hybridization width of the core-excited state has increased. Moreover, the energy positions of the C 1s maxima remain the same, whereas the O 1s peaks have moved slightly toward lower PEs. These observations support the interpretation that the remaining CO is adsorbed in sites with higher coordination, since, for example, previous results on CO/Ni(100) show a broadening of the XA peaks and a shift toward lower PE for the O 1s XA peak when increasing the coordination of the CO site.³¹

We will now discuss the XPS–XAS relationships. In the 2 Å case, the XPS BE appears near the XA onset, which was

also the case before heating. However, in the 0.2 Å case, the XPS BE has shifted to a position below the XA maximum. This can be taken as an indication for a change in the screening of the core ionized state. The XPS BE represents the energy required to create a core ionized CO ligand, screened by the surrounding Pd atoms, CO molecules, and oxide substrate. In particular, we consider two effects contributing rather effectively to the screening process. One is the coupling strength between the CO molecule and the deposited particle. The second is related to the size and polarizability of the electron reservoir, i.e., the extent of the system. This implies that screening is most effective for a metallic, strongly coupled adsorbate system. The screening processes for the species left after heating are nearly as efficient as for a metallic system, creating a core ionized state with an energy lower than the XA maximum. We attribute this to the larger CO–Pd hybridization strength and the smaller CO/Pd ratio, which would allow for a more efficient charge rearrangement upon ionization. In the case of CO saturation, however, the charge rearrangement in order to screen the core ionized site is less efficient, leading to a core ionized state with a higher energy than the neutral, core excited state, i.e., a more “molecularlike” behavior. The C 1s XPS peak at saturation coverage is thus shifted toward higher BE due to the less efficient screening as compared to the low coverage situation, i.e., the C 1s shift is largely caused by differences in the screening ability of the CO–Pd complex.

IV. CONCLUSIONS

Employing high resolution core level spectroscopies we have studied CO adsorption on Pd particles supported on a thin alumina film in detail. The studies revealed variations in the CO–Pd interaction depending on island size and CO coverage. Saturation coverage of CO at 90 K leads in all cases to an overlayer characterized in the core level spectra by a rather weak CO–Pd hybridization. The interaction strength gradually increases with island size. Desorption of 60% of the molecules results in an overlayer consisting of CO more strongly interacting with the Pd clusters. By comparing the XPS and XAS energies, information regarding the screening processes was obtained. A behavior indistinguishable from metallic systems was found for islands larger than 15 Å. For the smallest islands (about 5 Å), a CO coverage dependent XPS–XAS energy relation was observed: CO saturation yields a C 1s ionization energy larger than the energy required for the C $1s \rightarrow 2\pi^*$ excitation, whereas this relation is reversed after desorption of more than half of the CO overlayer. This indicates a drastically improved screening ability for the CO–Pd complex in the case of a low CO coverage.

ACKNOWLEDGMENTS

The authors thank J. N. Andersen for giving them access to the CO/Pd(111) data and the staff at MAX Lab for invaluable experimental assistance. This work was funded by the Deutsche Forschungsgemeinschaft, Ministerium für Wissenschaft und Forschung des Nordrhein–Westfalen, the Fonds der Chemischen Industrie, the Swedish Natural Science Re-

search Council (NFR), and the Swedish National Board for Industrial and Technical Development through the Consortium on Clusters and Ultrafine Particles. One author (A.S.) wishes to acknowledge NFR for a fellowship and a second author (J.L.) thanks the Studienstiftung des Deutschen Volkes for financial support.

- ¹G. Beitel, K. Markert, J. Wiechers, J. Hrbek, and R. J. Behm, in *Adsorption on Ordered Surfaces of Ionic Solids and Thin Films*, edited by H.-J. Freund and E. Umbach, Springer Series in Surface Science Vol. 33 (Springer, Berlin 1993).
- ²P. J. Chen and D. W. Goodman, *Surf. Sci.* **312**, L767 (1994).
- ³R. M. Jaeger *et al.*, *Surf. Sci.* **259**, 253 (1991).
- ⁴H.-J. Freund *et al.*, *J. Mol. Catalyt.* **82**, 143 (1993).
- ⁵F. Winkelmann *et al.*, *Surf. Sci.* **307-309**, 1148 (1994).
- ⁶J. Libuda, M. Bäumer, and H. J. Freund, *J. Vac. Sci. Technol. A* **12**, 2259 (1994).
- ⁷A. Sandell, J. Libuda, M. Bäumer, and H. J. Freund, *Surf. Sci.* **346**, 108 (1996).
- ⁸M. Bäumer *et al.*, *Ber. Bunsenges. Phys. Chem.* **99**, 1381 (1995).
- ⁹A. Sandell *et al.*, *J. Electron Spectrosc. Relat. Phenom.* (in press).
- ¹⁰X. Guo and J. T. Yates, Jr., *J. Chem. Phys.* **90**, 6761 (1989).
- ¹¹N. Mårtensson and A. Nilsson, in *Applications of Synchrotron Radiation*, edited by W. Eberhardt, Springer Series in Surface Science Vol. 35 (Springer, Berlin 1994), and references therein.
- ¹²J. N. Andersen *et al.*, *Synchrotron Rad. News* **4**, 21 (1991).
- ¹³J. N. Andersen *et al.* (unpublished).
- ¹⁴G. K. Wertheim, S. B. Di Cenzo, and D. N. E. Buchanan, *Phys. Rev. B* **33**, 5384 (1986).
- ¹⁵S. Kohiki, *Appl. Surf. Sci.* **25**, 81 (1986).
- ¹⁶T. Sarapatka, *J. Phys. Chem.* **97**, 11274 (1993).
- ¹⁷M. G. Mason, *Phys. Rev. B* **27**, 748 (1983).
- ¹⁸E. W. Plummer, W. R. Salaneck, and J. S. Miller, *Phys. Rev. B* **18**, 1673 (1978).
- ¹⁹H.-J. Freund and E. W. Plummer, *Phys. Rev. B* **23**, 4859 (1981).
- ²⁰K. S. Schönhammer and O. Gunnarsson, *Solid State Commun.* **23**, 691 (1977).
- ²¹K. S. Schönhammer and O. Gunnarsson, *Z. Phys. B* **30**, 297 (1978).
- ²²H. Antonsson *et al.*, *J. Electron Spectrosc. Relat. Phenom.* **54/55**, 601 (1987).
- ²³O. Björneholm *et al.*, *Surf. Sci.* **315**, L983. (1994).
- ²⁴H. Conrad, G. Ertl, and J. Küppers, *Surf. Sci.* **76**, 323 (1978).
- ²⁵F. M. Hoffman, *Surf. Sci. Rep.* **3**, 107 (1983).
- ²⁶J. N. Andersen *et al.*, *Phys. Rev. Lett.* **67**, 2822 (1991).
- ²⁷J. N. Andersen *et al.*, *Phys. Rev. B* **50**, 17525 (1994).
- ²⁸J. C. Fuggle *et al.*, *Solid State Commun.* **27**, 65 (1978).
- ²⁹H. Tillborg, A. Nilsson, and N. Mårtensson, *J. Electron. Spectrosc. Relat. Phenom.* **62**, 73 (1993).
- ³⁰Y. Jugnet, F. J. Himpsel, P. Avouris, and E. E. Koch, *Phys. Rev. Lett.* **53**, 198 (1984).
- ³¹O. Björneholm *et al.*, *Phys. Rev. B* **46**, 10353 (1992).
- ³²A. Nilsson *et al.*, *Chem. Phys. Lett.* **197**, 12 (1992).
- ³³O. Björneholm *et al.*, *Phys. Rev. Lett.* **68**, 1892 (1992).
- ³⁴H. Othani, M. A. Van Hove, and G. A. Somorjai, *Surf. Sci.* **187**, 372 (1987).